Journal of Nuclear Materials 377 (2008) 340–347

Contents lists available at ScienceDirect

Journal of Nuclear Materials

journal homepage: www.elsevier.com/locate/jnucmat

Determination of the E-pO^{2-} stability diagram of plutonium in the molten LiCl–KCl eutectic at 450 °C

Concha Caravaca [a,*], Annabelle Laplace [b], Jackie Vermeulen [b], Jérôme Lacquement [b]

[a] CIEMAT, DE/DFN/URR, Avda. Complutense 22, Madrid 28040, Spain
[b] Commissariat à l'Energie Atomique, Site de Marcoule, DEN/DRCP/SCPS/LPP, Bâtiment 399, BP 17171, 30207 Bagnols sur Cèze, France

ARTICLE INFO

Article history:
Received 11 September 2006
Accepted 30 January 2008

ABSTRACT

Plutonium trichloride solution in the molten LiCl–KCl eutectic was prepared by carbochlorination of plutonium oxide. Kinetics of this reaction was compared in different conditions in the range of 443–550 °C. Using this molten salt solution, the redox potential of the Pu(III)/Pu couple at inert tungsten electrode was measured at 450 °C by electromotive force measurement and was found to be $E'^{\circ} = -2.76$ V vs. the $Cl_{2(g)}$(1 atm)/Cl^- reference electrode (molar fraction scale). Reaction between plutonium trichloride and oxide ions was studied by potentiometric titration, using yttria stabilized electrodes. In our experimental conditions, the titration curves indicate the precipitation of the sesquioxide Pu_2O_3. The solubility product cologarithm calculated from these curves is found to be pK_s(Pu_2O_3) = 22.8 ± 1.1 (molality scale). Using the experimentally obtained values for E'°, activity coefficient and pK_s joined to the published thermodynamic data, the stability phase diagram of the Pu–O species was then drawn.

1. Introduction

An important criterion for future innovative reactor systems is the sustainability including minimization of waste output and its radiotoxicity. The most radiotoxic actinides (Pu, Np, Am, Cm) have a great impact, therefore their recycling is mandatory [1,2]. For homogeneous recycling of all actinides, pyrochemical process involving high-temperature, using molten salt and metal phases can be a promising alternative to the hydrometallurgical processes.

Over the last few years a lot of research has been carried out worldwide with the aim of separating these actinides and transmute them, in dedicated nuclear reactors, into stable or short-live radionuclides. The processes that are considered are both electrochemical processes (electrorefining and/or electrolysis) and reductive extraction. As molten salt media, chlorides and fluorides of alkali or alkaline-earth metals are under study. Some of the advantages of these molten salts processes are: their radiation resistance that allows a high actinide content in the medium and shorter cooling times, and their inherent proliferation resistance.

Special attention has been paid to the separation of actinides from rare-earths due to their similar chemical properties that make their separation quite difficult. Moreover, due to the neutronic poison effect of lanthanides, their allowed content in the future nuclear fuel has to be kept low.

In order to develop a future nuclear fuel cycle, the understanding of both chemical and electrochemical behaviour of actinides and lanthanides is essential, that includes a good knowledge of both thermodynamic and kinetics properties of the different elements involved in the process.

In molten salts, the chemical and electrochemical reactions that take place are influenced by the acidity of the media [3]. The Pourbaix type diagrams potential-oxoacidity, based on the definition of oxoacidity developed by Lux and Flood are useful to predict these reactions as they describe the behaviour of the different species in the selected molten salt in a summarising form. Considering this definition, the O^{2-} ions play the same role as the H^+ in aqueous media, according to which: oxoacid $+ O^{2-} \leftrightarrow$ oxobase. Thus, the oxoacidity of a solution can be measured in terms of $pO^{2-} = -\log a(O^{2-})$, being $a(O^{2-})$ the activity of the oxide ions.

There have been reported E-pO^2 diagrams for some rare earth elements in molten LiCl–KCl [4], there is less information about actinides (U, Np, Pu) in the same molten media [5].

The present work is part of an investigation concerning the chemical and electrochemical behaviour of plutonium in the molten LiCl–KCl eutectic. This paper deals with the preparation of Pu(III) solution from plutonium oxide and the identification of Pu–O stable species in this melt, which has been carried by potentiometric titrations of $PuCl_3$ solutions with the aid of O^{2-} ions selective electrodes. Also, the redox potential of the couple Pu(III)/Pu(0) is studied in order to establish the E-pO^{2-} diagram.

---

[*] Corresponding author. Tel.: +34 91 3466216; fax: +34 91 3466233.
E-mail address: c.caravaca@ciemat.es (C. Caravaca).

0022-3115/$ - see front matter © 2008 Elsevier B.V. All rights reserved.
doi:10.1016/j.jnucmat.2008.01.031

2. Experimental

2.1. General features

The molten electrolyte used in the experiments was the LiCl–KCl eutectic mixture (59 mol% LiCl, m.p. = 352°C) prepared from LiCl (Aldrich, >99.99% purity) and KCl (Aldrich, >99.999% purity). The LiCl–KCl eutectic was introduced either in a glassy carbon crucible (Carbone Lorraine, $Ø_{int}$ = 44 mm) or in a graphite crucible (Graphitec, ATJ49, $Ø_{int}$ = 45 mm). This was placed into a safeguard quartz crucible, itself into a sealed quartz cell, resistant to high-temperature and designed for electrochemical measurements. The cell was maintained under inert atmosphere with argon circulating through a quartz tube (Air Liquide, Ar N60, H_2O < 0.6 ppm, O_2 < 0.1 ppm). It was heated up to 200 °C for a few hours and then to the working temperature. The bath temperature was measured by a S type thermocouple (±1 °C) sheathed into a closed-end quartz tube (6–4 mm) immersed into the molten salt. Working temperature varied in the range 443–550 °C. Plutonium oxide, previously purified [6], was introduced with the salt in the crucible at the beginning of the experiment and dissolved by carbochlorination, introducing $Cl_{2(g)}$ in presence of graphite carbon.

2.2. Plutonium oxide carbochlorination

Plutonium chloride solution in LiCl–KCl melt was prepared using the carbochlorination technique, which reaction can be written as follows:

$$PuO_{2(s)} + C_{g(s)} + 2Cl_{2(g)} \rightarrow PuCl_4 + CO_{2(g)} \quad (1)$$

0.24–0.32 g of plutonium oxide were mixed with 35–48.3 g of LiCl–KCl eutectic and put in the crucible; which corresponds to 0.67 (±0.02) wt% of PuO_2 in the salt. Two sets of experiments were run. In the first one, carbochlorination was performed at 550 °C by bubbling $Cl_{2(g)}$ (Praxair, 99.99%) into the PuO_2–LiCl–KCl mixture, either in graphite or vitreous carbon crucible, at a volumetric flow rate of 2 l h^{-1} through a porous graphite tube (Carbone Lorraine, $Ø_{ext-int}$ = 8–4 mm, S = 4 cm^2 in the salt). At the top of the cell and outside the cell, the graphite tube was sheathed in a quartz tube to avoid any $Cl_{2(g)}$ leakage. The $Cl_{2(g)}$ that did not react was neutralized by a 5–6 M NaOH solution. In the second set of experiments, the reaction was performed under Cl_2 atmosphere in a closed reactor, without continuous bubbling. The LiCl–KCl eutectic was purified with $HCl_{(g)}$ previously to its introduction into the glovebox, PuO_2 powder was added and the bath melted. The chlorine reagent was passed at a flow rate of 2 l h^{-1} through the porous graphite tube during 30 min (with the first 15 min bubbling through the melt) in order to fully replace the $Ar_{(g)}$ atmosphere in the cell by a $Cl_{2(g)}$ one. The reaction cell was then closed and maintained under $Cl_{2(g)}$ atmosphere during at least 24 h. In order to increase the active reaction surface between $Cl_{2(g)}$ and graphite in the salt, two plates of graphite (Goodfellow, 99.95%, S_{tot} = 7.5 cm^2) were introduced into the melt. Experimental conditions are described in Table 1.

When the reaction was completed, argon was passed through the melt to release all $Cl_{2(g)}$ from the cell and the salt.

The kinetics of the PuO_2 conversion into plutonium chloride was carried out by taking samples of the molten bath. To avoid any $Cl_{2(g)}$ leakage and any air entry into the cell, samples were taken through an air lock under argon. Salt samples were then dissolved and diluted in 1 M HNO_3. The samples were filtered to avoid any undissolved PuO_2 particles. Plutonium chloride concentration was determined from the latter solutions by alpha counting and alpha spectrometry techniques. At the end of the dissolution, the plutonium concentration was about 2.4×10^{-2} mol kg^{-1}.

Table 1
Experimental carbochlorination conditions and results (atmosphere is noted atm)

Experiment	RunPu05	RunPu06	RunPu08	RunPu09	RunPu10
Gas condition	$Cl_{2(g)}$ bubbling	$Cl_{2(g)}$ bubbling	$Cl_{2(g)}$ atm	$Cl_{2(g)}$ atm	$Cl_{2(g)}$ atm
Temperature (°C)	550	550	443	500	545
Crucible nature	C_v	C_g	C_v	C_v	C_v
C_g-salt interface (cm^2)	4	42	7.5	7.5	7.5
PuO_2 weight (mg)	236	266	309	295	320
Salt weight (g)	35.01	40.01	45.01	45.23	48.31
Pu wt% if 100% dissolution	0.59	0.58	0.60	0.57	0.58
% of dissolution	99.2	97	94	99.3	97.3
Time needed (h)	4.5	3.3	30	≈7 (extrapolated)	6
Dissolution rate (mg of Pu/h)	48	75	11	38	44
Normalized dissolution rate (mg of Pu/g of salt/h)	1.3	1.8	0.2	0.8	0.9

2.3. Electrochemistry and potentiometric titration

Electrochemical study of $PuCl_3$ solutions in LiCl–KCl eutectic was performed using several transient electrochemical techniques such as cyclic voltammetry (CV) and open-circuit potentiometry (OCP). For the electrochemical measurements a three electrode set-up connected to a Potentiostat–Galvalnostat Autolab PG Stat 30 (Eco-Chemie) was used.

Working and counter electrodes used in all the experiments consisted of a 1 mm diameter tungsten wire (Goodfellow, 99.99%). The reference electrode was made of a silver wire (1 mm Ø, Goodfellow, 99.99%) dipped into a closed-end Pyrex glass tube containing a 0.75 mol kg^{-1} silver chloride (Aldrich, 99%) solution in LiCl–KCl eutectic.

For the potentiometric titrations, the electrodes used consisted of a AgCl/Ag reference electrode, above described, and a selective oxide ions membrane electrode. The latter, is constituted by a closed-end tube of ZrO_2 stabilised with Y_2O_3 (8%), containing a constant O^{2-} ion concentration, 0.1 mol kg^{-1} in LiCl–KCl, introduced as solid Li_2CO_3 (Aldrich 97%) and an internal AgCl/Ag reference. Two different electrodes have been tested and compared; both containing a 8% of Y_2O_3; the first one, was a 4–6 mm tube from OMG (France) and the second one was a 6–8 mm tube from Interbil S.A. (Spain).

Potentiometric titrations were performed measuring the e.m.f. between the reference and the YSZE electrodes after adding known amounts of O^{2-} ions, introduced as solid Li_2CO_3 (Aldrich, 99%) or BaO (Aldrich, 97%); then, $Ar_{(g)}$ was bubbled into the melt.

3. Results and discussion

3.1. Plutonium solution preparation

3.1.1. Carbochlorination reaction

Except at 443 °C with 94% dissolution, more than 97% dissolution of the initial PuO_2 was reached and we can consider that the dissolution is total. Sampling during the dissolution and analytical errors leads to a more difficult mass balance. During the dissolution, while there was chlorine gas in the molten solution, the salt was green. After the dissolution was completed, chlorine gas was evacuated by argon, and the Pu(IV) that is stable only in chlorine atmosphere [5] was reduced to Pu(III) obtaining a blue solution:

$$PuCl_4 \rightarrow PuCl_3 + 0.5Cl_{2(g)} \quad (2)$$

Fig. 1 shows a typical cyclic voltammogram of the plutonium solution obtained after carbochlorination and under $Ar_{(g)}$ atmosphere at 450 °C. The electroactivity domain in LiCl–KCl is limited by the Li^+/Li and the $Cl_{2(g)}/Cl^-$ redox systems, in reduction and oxidation, respectively. Its experimental width is about 3.71 V which is consistent with the theoretical value of 3.68 V calculated from the thermodynamic values for pure compounds and Li^+ ion activity in the LiCl–KCl eutectic at 450°C [7,8]. Except those two former redox systems, there is only another one. The cathodic peak Ic at a potential of −1.92 V vs. AgCl/Ag and its corresponding anodic peak I_A ($E_p = -1.76$ V vs. AgCl/Ag) were attributed to the reduction of Pu(III) ions into Pu metal and to the reoxidation of Pu(0) into Pu(III), respectively. The shape of the anodic peak is characteristic of the dissolution of an insoluble phase deposited on the electrode during the forward scan (stripping peak) [9]. The potential value of the cathodic peak is consistent with the reported values in the literature [10].

3.1.2. Dissolution kinetics

The different results are summarised in Table 1. The plutonium concentration after complete dissolution is roughly the same for each experiment (between 0.57 and 0.6 wt% of Pu(III) in the salt). The dissolution rate has been calculated from the rising part of the dissolution curve before complete dissolution was reached (Fig. 2). In order to take in account the small variations of initial mass of salt, we have normalized the dissolution rate per g of salt.

3.1.2.1. Carbochlorination under circulating $Cl_{2(g)}$. Based on previous experiments, we limited the study to the temperature of 550 °C. Higher temperatures would lead to an important evaporation of the salt.

The dissolution rate by carbochlorination under our experimental conditions is in the range of 1–2 mg of Pu/g of salt/h. Compared to previous dissolution experiment of PuO_2 in the same eutectic with $HCl_{(g)}$ (Eq. (3)), which dissolution rate was around 0.2 mg of Pu/g of salt/h, kinetics are better,

$$PuO_2 + 4HCl_{(g)} \rightarrow PuCl_3 + 2H_2O_{(g)} + 1/2Cl_{2(g)} \tag{3}$$

The standard free energies of those two dissolution reactions show that the carbochlorination is much more favourable (Table 2) [11].

Increase of graphite surface area allows to accelerate the reaction. However, the use of a graphite crucible is not convenient from an experimental point of view: there are C_g particles in the salt and at the end of the experiment the frozen salt cannot be removed from the crucible.

Despite the increase of the graphite surface area, kinetics of the reaction remain slow and this is attributed to the low solubility of chlorine gas in molten salts. Table 3 shows chlorine gas solubility and diffusion coefficient in LiCl–KCl eutectic at different temperatures [12,13]. The values of diffusion coefficients are one order of magnitude higher than those found for metallic ions in the same molten salt media, which are about 10^{-5} $cm^2\,s^{-1}$. The solubilization of chlorine gas in the molten salt is written as follows:

$$Cl_{2(g)} \leftrightarrow Cl_{2(salt)} \tag{4}$$

Its equilibrium constant K_{eq} (mol cm^{-3} atm) is expressed as

$$K_{eq} = \frac{[Cl_2]_{(salt)}}{P_{Cl_{2(g)}}} \tag{5}$$

$[Cl_2]_{(salt)}$ (mol cm^{-3}) being the concentration of dissolved chlorine and $P_{Cl_{2(g)}}$ (atm), the chlorine gas pressure above the molten salt. For the calculation of $[Cl_2]_{(salt)}$ in our experiments we have considered a pressure of 1 atm. It increases with the temperature and contrary to the diffusion coefficient; the chlorine solubility is low which would explain the observed low kinetics.

For both dissolution experiments performed under circulating chlorine gas, less than 1% of chlorine gas had indeed reacted with plutonium oxide. The other 99% was not necessary and was captured by the NaOH solution.

In order to reduce the volume of NaOH solutions used and waste produced, carbochlorination was run under Cl_2 atmosphere in a closed reactor.

3.1.2.2. Carbochlorination under closed $Cl_{2(g)}$ atmosphere. The temperature effect was tested from 450 to 550 °C and in all cases complete dissolution was reached.

The quantity of chlorine gas in the cell (≈800 ml) was largely enough compared to the PuO_2 amount to be dissolved. Fig. 2 shows the solubilization curves at the different temperatures. Temperature increase accelerates the kinetics in particular from 443 to 500 °C. This is consistent with chlorine solubility and diffusion coefficient in molten LiCl–KCl (Table 3). Also thermodynamics become slightly more favourable with the temperature (Table 2).

At 550 °C, kinetics is slightly slower for the dissolution under chlorine atmosphere rather than continuous chlorine gas bubbling in the salt. The carbochlorination reaction (1) shows that a mole of $CO_{2(g)}$ is produced for two moles of $Cl_{2(g)}$ consumed. Therefore, for

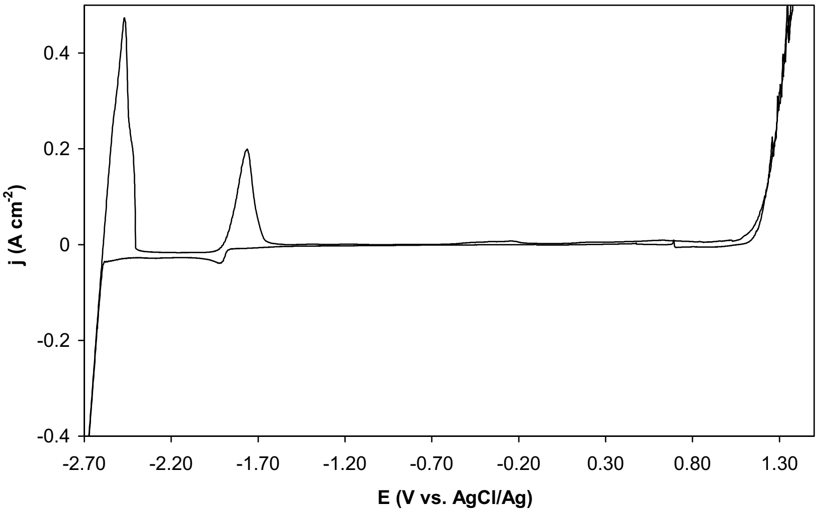

Fig. 1. Cyclic voltammogram of the LiCl–KCl–Pu(III) solution on a tungsten electrode at 450 °C, $v_{scan} = 0.1$ V s^{-1}, $[Pu(III)] = 2.4 \times 10^{-2}$ mol kg^{-1}.

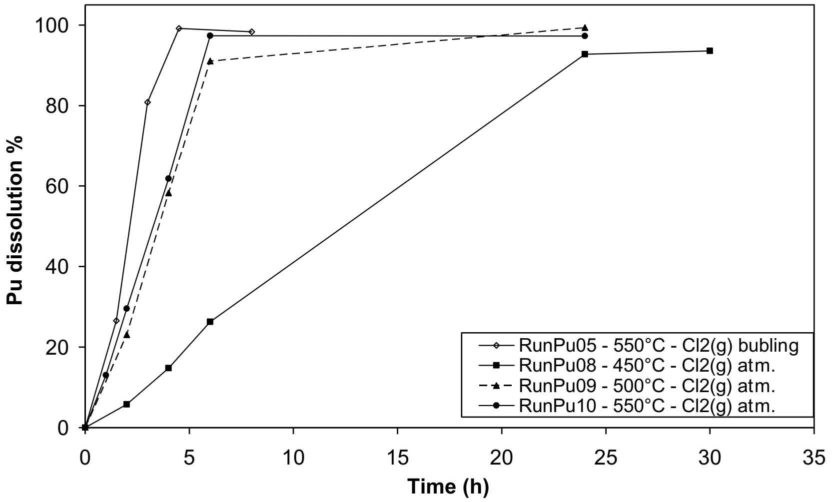

Fig. 2. Evolution of the percentage of PuO_2 dissolved in LiCl–KCl at different temperatures, under circulating and closed $Cl_{2(g)}$ atmosphere.

Table 2
Free energy of reaction for pure compounds (kJ mol^{-1}) [11]

Temperature (°C)	450	500	550
ΔG_f° (kJ mol^{-1})			
$PuO_{2(s)} + C_{g(s)} + 2Cl_{2(g)} \rightarrow PuCl_4 + CO_{2(g)}$	−206	−211	−215
ΔG_f° (kJ mol^{-1})			
$PuO_2 + 4HCl_{(g)} \rightarrow PuCl_3 + 2H_2O_{(g)} + 1/2Cl_{2(g)}$	100	108	116

Table 3
Chlorine gas solubility (at 1 atm) and diffusion coefficient in LiCl–KCl eutectic

Temperature (°C)	K_{eq} (mol cm^{-3} atm^{-1}) [12]	$[Cl_2]_{(salt)}$ (at 1 atm) (mol kg^{-1})	Diffusion coefficient (cm^2 s^{-1}) [13]
400	1.26×10^{-7}	7.53×10^{-5}	6.00×10^{-5}
450	1.54×10^{-7}	9.34×10^{-5}	1.60×10^{-4}
500	1.70×10^{-7}	1.05×10^{-4}	1.70×10^{-4}
550	2.05×10^{-7}	1.29×10^{-4}	1.50×10^{-4}

the first method, there is a slight accumulation of $CO_{2(g)}$ in the cell, the chlorine gas pressure decreases and the chlorine solubility in the molten eutectic also decreases. For the second method some salt agitation is also provided by the gas bubbling. Both parameters could explain the small kinetics difference.

3.2. Determination of E-pO^{2-} stability diagram of Pu

The stability domain of the Pu–O compounds in the molten LiCl–KCl eutectic can be defined by the potential – pO^{2-} equilibrium diagrams according to Trémillon [3]. The construction of these diagrams is based on both experimental and thermodynamic data of redox potentials and solubility products. According to the definition of oxoacidity–oxobasicity defined by Lux and then by Flood [14,15], it is possible to determine the nature of the Pu–O compounds and their solubility products by potentiometric titrations using oxide ions.

Data of the Pu_2O_3 solubility product and standard potential of the Pu(III)/Pu(0) redox couple used in the construction of the diagram presented here have been determined experimentally and will be detailed in the following sections.

3.2.1. Apparent standard redox potential of Pu(III)/Pu(0) determination

The apparent standard potential of the Pu(III)/Pu(0) redox couple was determined by e.m.f. measurements of the galvanic cell: Pu(0)|LiCl–KCl–$PuCl_3$||AgCl, LiCl–KCl|Ag(0), at 450 °C, by using the open-circuit chronopotentiometry technique. Plutonium metal was electrodeposited in situ; a cathodic potential was applied for 30–60 s at a tungsten electrode, and then potential at open-circuit was recorded vs. time, see Fig. 3. From the pseudo-equilibrium potential measured at the plateau observed in this figure, the apparent standard potential of the redox couple was determined using the Nernst equation:

$$E_{Pu(III)/Pu(0)} = E'^{\circ}_{Pu(III)/Pu(0)} + \frac{2.3RT}{nF}\log X_{PuCl_3} - E^{\circ}_{Ag(I)/Ag(0)} + \frac{2.3RT}{nF}\log X_{AgCl} \tag{6}$$

Being the apparent standard potential, E'°, equal to:

$$E'^{\circ}_{Pu(III)/Pu(0)} = E^{\circ}_{Pu(III)/Pu(0)} + \frac{2.3RT}{nF}\log \gamma_{PuCl_3} \tag{7}$$

Potential measurements were performed vs. the AgCl/Ag reference electrode and then transformed into values vs. the $Cl_{2(g)}$(1 atm)/Cl^- reference electrode. For a AgCl (0.75 mol kg^{-1})/Ag reference electrode, the expression used was the following [15]:

$$E(AgCl/Ag) = -1.244 + 2.6710^{-4} \cdot T \tag{8}$$

Potentials are expressed in volts and temperature in Kelvin degrees. At 450°C, the theoretical value is −1.051 V.

The apparent standard potential value of the Pu(III)/Pu(0) redox couple obtained this way at 450 °C was −2.76 V vs. $Cl_{2(g)}$(1 atm)/Cl^- in mole fraction scale.

From the difference of the Gibbs free energy of $PuCl_3$ formation, calculated from the experimental value of $E'^{\circ}_{(Pu(III)/Pu(0))}$, and the Gibbs free energy of $PuCl_3$ formation of pure compounds using as reference the supercooled liquid state taken from the literature [10], the activity coefficient of $PuCl_3$ in LiCl–KCl at 450 °C was determined using the following expression:

$$\log \gamma = \frac{\Delta G'^{\circ}(\exp) - \Delta G^{\circ}(sc)}{2.3RT} \tag{9}$$

The value of $\log \gamma$ obtained was equal to −1.59; this value indicates that the Pu(III) ions are solvated by the Cl^- ions of the melt, which in turn means a stabilization of the Pu(III) ions in the LiCl–KCl.

3.2.2. $PuCl_3$ solution titration

In order to determine the nature and stability of Pu–O compounds formed in the LiCl–KCl eutectic, titrations of solutions

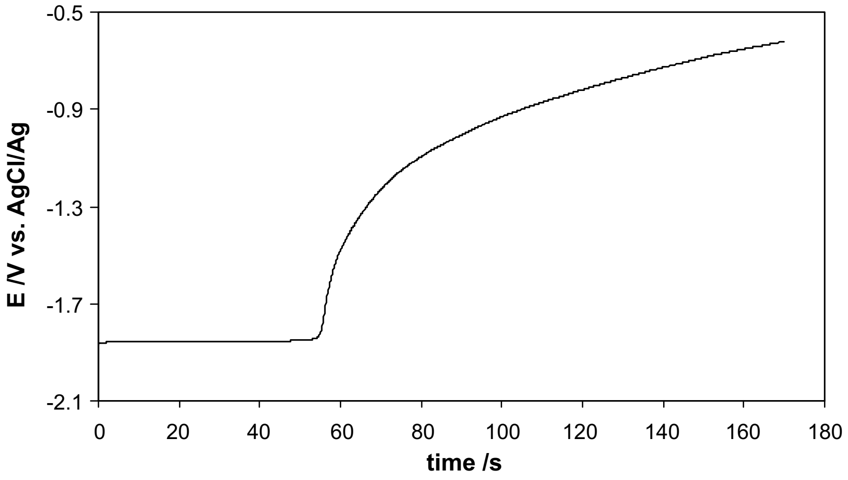

Fig. 3. Chronopotentiogram obtained at a tungsten working electrode at 450 °C by imposing a potential of −1.865 V vs. AgCl/Ag, for 30 s. [Pu(III)] = 2.0 × 10^{-2} mol kg^{-1}.

containing $PuCl_3$, at an initial concentration of 1.0 × 10^{-2} mol kg^{-1}, were performed by adding small amounts of lithium carbonate as O^{2-} donor. In these titrations the two different YSZ electrodes used, as indicated previously, were introduced in the same Pu(III) solution in order to compare the results.

The titration is based on the definition of pO^{2-} (=$-\log a(O^{2-})$) and is performed using an electrode that is selective for free oxide ions in the solution. This electrode is constituted by a membrane of zirconia stabilised with yttria (YSZE) and its response presents a nernstian behaviour in this melt, according to the equation [16]:

$$E = E^{\circ} + \frac{2.3RT}{2F} pO^{2-} \tag{10}$$

Before its use, the nernstian behaviour of the electrodes was checked performing potentiometric titrations of the LiCl–KCl melt with O^{2-} ions introduced either as solid BaO or Li_2CO_3. The titration also allowed determining the $E^{\bigcirc}$ value of Eq. (5). The pO^{2-} values used for the electrode calibration varied between 1 and 2. In this range, the variation of the YSZE potential as a function of the pO^{2-} is linear and the slope is close to the theoretical value of 0.072 corresponding to an exchange of 2 electrons ($O_{2(g)}/O^{2-}$ redox system). This can be observed in Fig. 4 for calibration of both electrodes (Interbil and OMG) performed with BaO additions.

As the $E^{\bigcirc}$ value slightly changes in each titration, the electrode calibration was also performed for each experiment taking the last points of the plutonium titration curve, when practically all of the plutonium has precipitated and the potential scarcely changes with the successive additions of O^{2-} ions.

The titration curve of Fig. 5 shows an equivalent point for an α value of 1.5, being α equal to the ratio of added O^{2-} ions concentration to initial Pu(III) concentration, C_0: $\alpha = [O^{2-}]_{add}/[Pu^{3+}]_{ini}$. The value of α equal to 1.5 corresponds to the formation of Pu_2O_3 according the following reaction:

$$2Pu^{3+} + 3O^{2-} \leftrightarrow Pu_2O_3 \tag{11}$$

Its solubility product being expressed as:

$$K_s(Pu_2O_3) = [Pu^{3+}]^2[O^{2-}]^3 \tag{12}$$

The same response was observed in all the titrations performed with both YSZ electrodes. In the experimental conditions used in this work, no evidences of plutonium oxychloride precipitation were observed. However, in the titration curve it is observed at the early stages of the process a decrease of the pO^{2-}, for $0 < \alpha < 0.3$. Similar behaviour has also been observed for several authors, Lambertin [17] for Am(III) in LiCl–KCl at 450°C, and Combes et al. [18] for the Ce(III) in NaCl–KCl at 720°C. In all these cases

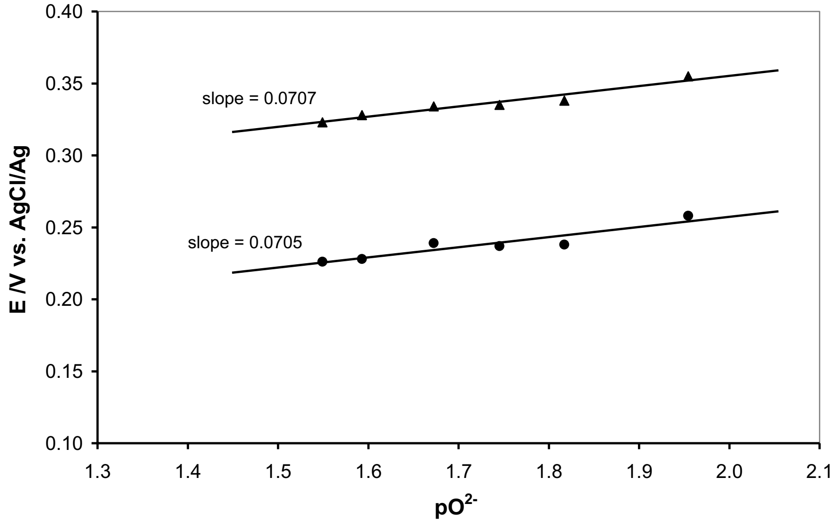

Fig. 4. Experimental calibration of the YSZ electrodes by BaO additions in LiCl–KCl at 450°C. (●) Interbil S.A. and (▲) OMG.

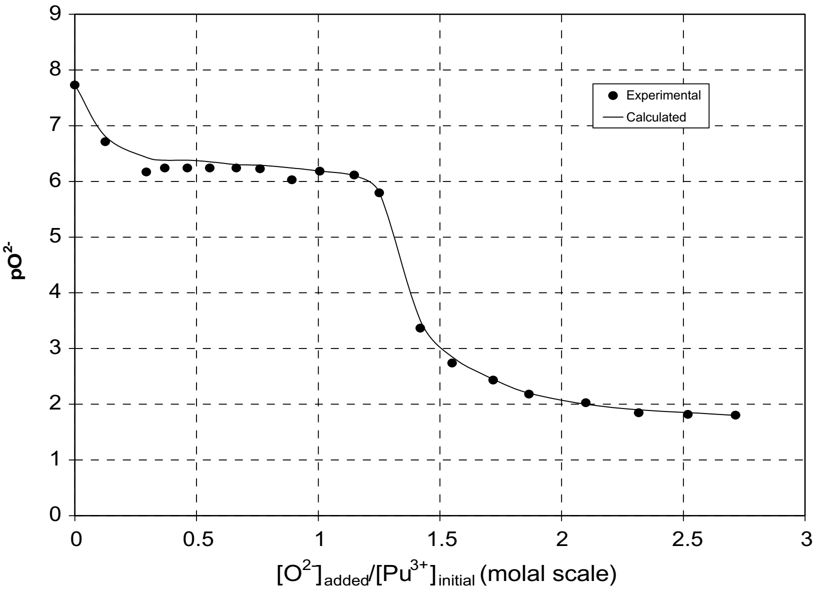

Fig. 5. (●) Experimental and (line) calculated potentiometric titration curve of a solution containing Pu(III) at a concentration of 1.0×10^{-2} mol kg^{-1} in LiCl–KCl at 450 °C by O^{2-} ions added as solid Li_2CO_3, performed with an YSZE electrode from Interbil S.A.

the decrease of pO^{2-} was attributed to the formation of a soluble oxychloride compound, AmO^+ or CeO^+, respectively. Cherginets indicates that this sharp pO^{2-} decrease in the initial section of the potentiometric curve is produced because the initial oxide ion concentration in the melt is not enough to achieve the solubility product at that stage [19].

Based on these works, authors thinks that the sharp decrease of pO^{2-} observed in the early stages of the curve, could be due to the soluble plutonium oxychloride, PuO^+, formation.

Determination of the plutonium sesquioxide solubility product, $K_s(Pu_2O_3)$, in molality scale, was performed from the analysis of the titration curves for both YSZ electrodes. For plutonium, the following mass balance equation can be written:

$$C_0 = [Pu^{3+}] + \left[\frac{2nPu_2O_3}{m}\right] \tag{13}$$

where C_0 is the initial concentration (in mol kg^{-1}), as indicated previously, nPu_2O_3 is the number of Pu_2O_3 moles and m the LiCl–KCl mass. Concentrations are all expressed in molality scale. For oxide ions, using α previously defined, it is obtained:

$$\alpha C_0 = [CO_3^{2-}] + [O^{2-}] + \left[\frac{3nPu_2O_3}{m}\right] \tag{14}$$

The solubility product corresponding to reaction (11) is given by the expression (12). The free oxide ion concentration in the melt depends also on the carbonate dissociation equilibrium:

$$CO_3^{2-} \leftrightarrow CO_{2(g)} + O^{2-} \tag{15}$$

The equilibrium constant of this reaction is given by the following expression:

$$K_d = \frac{P(CO_2)[O^{2-}]}{[CO_3^{2-}]} \tag{16}$$

Despite some authors such as Cherginets consider that the dissociation of carbonates is not complete unless the atmosphere inside the cell is free of $CO_{2(g)}$ [20], Combes et al. [21] in NaCl–KCl, Séon [16] and Picard et al. [22], in LiCl–KCl, have proved that the dissociation is complete as long as the partial pressure of $CO_{2(g)}$ remains below 10^{-3} atm; this can be easily achieved bubbling an inert gas, $Ar_{(g)}$, into the melt.

For the titration curve, the following expression can be derived:

$$\alpha = \frac{3}{2} + \frac{1}{C_0}\left\{[O^{2-}]\left(\frac{P(CO_2)}{K_d} + 1\right) - \frac{3}{2}\left(\frac{K_s(Pu_2O_3)}{[O^{2-}]^3}\right)^{1/2}\right\} \tag{17}$$

The solubility product was calculated fitting the experimental points of the curve obtained during the Pu(III) titration before the equivalent point, and taking the average value of these values. In these conditions the first two terms of expression (17) are negligible and the expression can be simplified as follows:

$$pO^{2-} = -\frac{1}{3}\log\left(\frac{K_s(Pu_2O_3)}{C_0^2(1-\frac{2}{3}\alpha)^2}\right) \tag{18}$$

The average value of the $pK_s(Pu_2O_3)$ obtained at 450 °C, considering values obtained with the two electrodes, is 22.8 ± 1.1 (molality scale), see Table 4. This result can be compared to that of Martinot and Fuger [23] that obtained the value of 26.5 ± 3 (molality scale) by titration in LiCl–KCl at 450 °C. Also the value determined by potentiometric titration is in good agreement to that obtained from thermochemical data, which can be calculated using the constant related to the following equilibrium between pure compounds:

$$Pu_2O_{3(s)} + 6LiCl(l) \overset{K^*}{\leftrightarrow} 2PuCl_3(l) + 3Li_2O(l) \tag{19}$$

According to Mottot [15], the solubility product can be determined using the expression:

$$pK_s(Pu_2O_3) = pK^* - 6\log a_{LiCl} + 2\log\gamma_{Pu^{3+}} + 3\log\gamma_{Li_2O} \tag{20}$$

The value of K^* is calculated from the thermochemical data of solid pure compounds obtained from the literature [24]. The value of $\log\gamma(Pu^{3+}) = -1.59$ was experimentally determined, as indicated previously. The activity of the LiCl in LiCl–KCl, that was obtained

Table 4
Experimental values of the solubility product of Pu_2O_3 obtained at 450 °C

Electrode	$K_s(Pu_2O_3)$	$pK_s(Pu_2O_3)$	Average value	Theoretical $pK_s(Pu_2O_3)$
OMG	1.0×10^{-22}	22.0	22.8 ± 1.1	23.0
Interbil S.A.	3.16×10^{-24}	23.5		

Table 5
Equilibrium potential and values of standard potentials of the Pu redox systems in LiCl–KCl eutectic at 450 °C

Redox system	Equilibrium potential expression	Standard potential /V vs. Cl_2(1 atm)/Cl^-
$Pu^{3+} + 3e^- \leftrightarrow Pu(s)$	$E = E_1^\circ + \frac{2.3RT}{3F}\log[Pu^{3+}]$	$E_1^\circ = -2.83$
$Pu_2O_{3(s)} + 6e^- \leftrightarrow 2Pu_{(s)} + 3O^{2-}$	$E = E_2^\circ + \frac{2.3RT}{2F}pO^{2-}$	$E_2^\circ = E_1^0 - \frac{2.3RT}{6F}pK_s(Pu_2O_3) = -3.37$
$PuO_2(s) + e^- \leftrightarrow Pu^{3+} + 2O^{2-}$	$E = E_3^\circ - \frac{2.3RT}{F}\log[Pu^{3+}] + \frac{2x2.3RT}{F}pO^{2-}$	$E_3^0 = -4.50$
$2PuO_{2(s)} + 2e^- \leftrightarrow Pu_2O_{3(s)} + O^{2-}$	$E = E_4^\circ + \frac{2.3RT}{2F}pO^{2-}$	$E_4^\circ = E_3^\circ + \frac{2.3RT}{2F}pK_s(Pu_2O_3) = -2.86$

Molality scale. [Pu(III)] = [Pu(IV)] = 1.0×10^{-2} mol kg^{-1}.

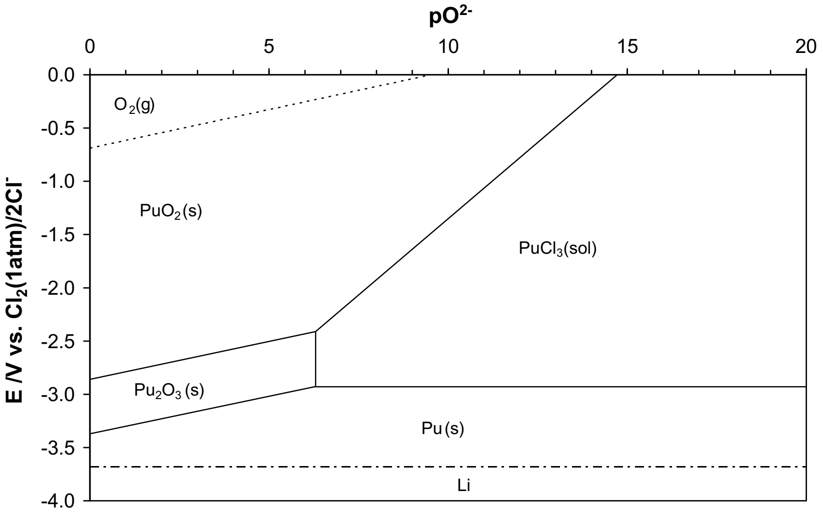

Fig. 6. Potential-pO^{2-} diagram for plutonium in LiCl–KCl eutectic at 450 °C and [Pu(III)] = [Pu(IV)] = 1.0×10^{-2} mol kg^{-1}.

from the literature, is a(LiCl) = 0.364 at 450 °C [8]. Activity coefficient of Li_2O, $\gamma(Li_2O)$, that can be calculated according to the method described by Séon [16] has a value of $\log\gamma(Li_2O) = -5.16$ at 450 °C [24]. Using Eq. (16) and these values, the value of $pK_s(Pu_2O_3)$ is equal to 23.0, in molality scale, which is very close to the one determined here experimentally.

3.2.3. *E-pO^{2-} diagram construction*

The construction of the E-pO^{2-} diagram of plutonium in molten LiCl–KCl eutectic at 450°C, for a concentration of 1.0×10^{-2} mol kg^{-1}, was performed using the equilibrium potentials expressions corresponding to the different redox systems indicated in Table 5, joined to the $K_s(Pu_2O_3)$ value. The apparent standard potential of the Pu(III)/Pu(0) redox couple, Pu(III) activity coefficient and Pu_2O_3 solubility product values were determined experimentally. The other values were obtained from literature thermochemical data.

It is not possible to prepare a solution of Pu(IV) under $Ar_{(g)}$ atmosphere, since the Pu(IV) is reduced by the chloride ions of the melt producing Pu(III) [5,23]. For this reason, the standard potential of the redox couple $PuO_{2(s)}$/Pu(III), E_3^0, has been calculated from the published thermochemical data [24] and the experimental value of the $PuCl_3$ activity coefficient, indicated previously. For the calculation it has also been used the value of the constant for pure compounds, K^*, concerning the equilibrium:

$$PuO_2(s) + 4LiCl(l) \leftrightarrow PuCl_3(l) + 2Li_2O(l) + \frac{1}{2}Cl_2 \tag{21}$$

According to Séon [16] and Lambertin et al. [25], the value of the standard potential E_3^0 of the $PuO_{2(s)}$/Pu(III) redox system can be determined using the following expression:

$$E_3^\circ = \frac{2.3RT}{F}\left[\log K^* + 4\log a_{LiCl} - \log\gamma_{Pu^{3+}} - 2\log\gamma_{Li_2O}\right] \tag{22}$$

where K^* is calculated using the thermochemical data obtained from the literature [24]. Li_2O activity coefficient and the LiCl activity were given before. Standard potential value of the $PuO_{2(s)}$/Pu(III) redox couple calculated this way is equal to −4.50 V vs. Cl_2(1 atm)/Cl^- as indicated in Table 5.

Using this value, the standard potential value of the Pu(III)/Pu redox couple, already given, and the Pu_2O_3 solubility product also determined experimentally in this work (the average value is $10^{-22.8}$), the potential-pO^{2-} diagram of Fig. 6 was drawn. Relations between potentials and pO^{2-} used to construct this diagram are given in Table 5.

The pO^{2-} diagram of plutonium in molten LiCl–KCl allows predicting the chemical and electrochemical reactions of Pu in this molten salt media a 723 K. The obtained diagram shows similar plutonium compound domains to those observed by Martinot in LiCl–KCl eutectic at 723 K [23] and Lambertin in NaCl–$CaCl_2$ at 823 K [25].

4. Conclusions

This work focused on plutonium(III) chloride solutions preparation and the construction of the E-pO^{2-} diagram of plutonium in molten LiCl–KCl eutectic at 450 °C.

Plutonium dioxide powder was converted into plutonium trichloride by carbochlorination. This method was shown to be efficient although kinetics was found to be quite low. This was attributed to the low chlorine solubility in the molten LiCl–KCl eutectic. In order to reduce the amount of chlorine gas which had not reacted and was captured at the exit of the reaction cell, carbochlorination was performed under $Cl_{2(g)}$ atmosphere in a closed reactor. This is efficient with our plutonium quantities to be dissolved.

The Pu(III)/Pu redox potential was determined at inert electrode by electromotive force measurement and the Pu(III) activity coefficient shows a complexation of the Pu(III) in the molten bath.

Solubility product of Pu–O compounds was determined by potentiometric titrations. The plot of pO^{2-} as a function of α being the ratio: $\alpha = [O^{2-}]_{add}/[Pu^{3+}]_{ini}$, shows a single equivalent point for α equal to 1.5. This indicates the precipitation of Pu_2O_3 in the molten LiCl–KCl. The solubility product was determined from the titrations curves and the average value obtained for its cologarithm is: $pK_s(Pu_2O_3) = 22.8 \pm 1.1$ (molality scale). The beginning of the curve also suggests the formation of the soluble PuO^+ specie.

The stability phase diagram of the Pu–O species in the eutectic LiCl–KCl at 450 °C, in molality scale, was drawn using the experimentally obtained values for $E°$, pK_s, and activity coefficient joined to the published thermodynamic data. Although thermodynamic data predict the precipitation of plutonium oxychloride; PuOCl, this was not observed in our experimental conditions. Pu(III) species are stabilized by complexation in LiCl–KCl, which produces a shift of the stability domain of the plutonium trichloride to smaller pO^{2-} values, which means a reduction of the PuOCl domain.

Acknowledgements

This work has been carried out at CEA (Marcoule) under the CEA-CIEMAT agreement (C4974f). The investigation is also part of the CIEMAT-ENRESA agreement for the development of activities in the ‘Partitioning and Transmutation’ field. Authors wish to thank the laboratory staff in Atalante (CEA, Marcoule) for their technical support.

References

[1] OCDE/NEA, Actinide and Fission Product Partitioning and Transmutation, Status and Assessment Report, 1999.
[2] OCDE/NEA, Accelerator-Driven Systems (ADS) and Fast Reactors (FR) in Advanced Nuclear Fuel Cycles, A Comparative Study, 2002.
[3] B. Trémillon, Pure Appl. Chem. 25 (1971) 395.
[4] H. Hayashi, K. Minato, J. Phys. Chem. Solids 66 (2–4) (2005) 422.
[5] L. Martinot, in: A.J. Freeman, C. Keller (Eds.), Handbook of the Physics and Chemistry of Actinides, vol. 6, North Holland, 1991, p. 241 (Chapter 4).
[6] A.G. Osipenko, P.T. Porodnov, O.V. Skiba, A.V. Bychkov, L.G. Babikov, J. Lacquement, Ph. Brossard, J. Bourges, B. Sicard, in: 5th International Symposium on Molten Salt Chemistry and Technology Proceedings, Dresde, Germany, 1997, p. 533.
[7] I. Barin, Thermochemical Data for Pure Substances, VCH Verlags Gesellshaft, Weinheim, 1993.
[8] J. Lumsden, Thermodynamics of Molten Salt Mixtures, Academic Press, New York, 1966.
[9] A.J. Bard, L.R. Faulkner, Electrochemical Methods: Fundamentals and Applications, John Wiley, New York, 1980.
[10] J.J. Roy, L.F. Grantham, D.L. Grimmet, S.P. Fusselman, C.L. Krueger, T.S. Storvick, T. Inoue, Y. Sakamura, N. Takahashi, J. Electrochem. Soc. 143 (8) (1996) 2487.
[11] (a) I. Barin, Thermochemical Data for Pure Substances, VCH Verlags Gesellshaft, Weinheim, 1989;
(b) I. Barin, O. Knacke, O. Kubaschewski, Thermodynamic Properties of Inorganic Substances, Springer-Verlag, Berlin/New York, 1977. Suppl.;
(c) O. Knacke, O. Kubaschewski, K. Hesselman, Thermochemical Properties of Inorganic Substances, 2nd Ed., Springer-Verlag, Berlin, 1991. pp. 1114–2412.
[12] L.E. Ivanovski, V.N. Nekrasov, The Gases and Ionic Melts, M. Nauka, Moscow, 1979.
[13] J.D. Van Norman, R.I. Tivers, in: G. Mamantov (Ed.), Molten Salts, Marcel Dekker, New York, 1969, p. 509.
[14] H. Flood, T. Förland, Acta Chem. Scandinavica 1 (1947) 592.
[15] Y. Mottot, PhD Thesis, Propriétés chimiques et électrochimiques des chlorures de lanthanides cériques en milieux chlorures fondus. Stabilité thermodynamique des alliages La-Ni et Nd-Fe à haute température. Université Pierre et Marie Curie, Paris VI, 1986.
[16] F. Séon, PhD Thesis, Réaction d’échange de l’ion oxyde dans l’eutectique LiCl–KCl à 470° C. Application à la chloruration sélective d’oxydes métalliques en milieu chlorures fondus. Département Sciences Physiques, Université Pierre et Marie Curie, Paris VI, 1981.
[17] D. Lambertin, PhD Thesis, Propriétés chimiques de l’américium dans l’eutectique LiCl–KCl fondu. Application à la séparation américium-lanthanides (néodyme). Université Pierre et Marie Curie, Paris VI, 2001.
[18] R. Combes, M.N. Levelut, B. Trémillon, J. Electroanal. Chem. 91 (1978) 125.
[19] V.L. Cherginets, O.V. Menirskaya, T.P. Rebrova, CPS: physchem/0203001 (2002) 1–4.
[20] V.L. Cherginets, Electrochim. Acta 42 (23–24) (1997) 3619.
[21] R. Combes, R. Feys, B. Trémillon, J. Electroanal. Chem. 83 (1977) 383.
[22] G. Picard, F. Seon, B. Trémillon, J. Electroanal. Chem. 102 (1979) 65.
[23] L. Martinot, J. Fuger, J. Less-Common Metals 120 (1986) 255.
[24] I. Barin, O. Knacke, Thermochemical Properties of Inorganic Substances, Springer-Vergal, Berlin, 1973.
[25] D. Lambertin, J. Lacquement, S. Sanchez, G. Picard, Electrochem. Commun. 4 (2002) 447.